Submarine mass-wasting on glacially-influenced continental slopes: processes and dynamics

ANDERS ELVERHØI[1], FABIO V. DE BLASIO[1,2], FAISAL A. BUTT[1,6], DIETER ISSLER[3], CARL HARBITZ[2], LARS ENGVIK[4], ANDERS SOLHEIM[2], & JEFFREY MARR[5]

[1]*Department of Geology, University of Oslo, P.O. Box 1047, Blindern, N-0316 Oslo, Norway (e-mail: anders.elverhoi@geologi.uio.no)*

[2]*Norwegian Geotechnical Institute, P.O. Box 3930, Ullevål Stadion, N-0806 Oslo, Norway*

[3]*NaDesCoR, Promenade 153, CH-7260 Davos Dorf, Switzerland*

[4]*Sør-Trøndelag University College, N-7004 Trondheim, Norway*

[5]*St Anthony Falls Laboratory, University of Minnesota, Mississippi River at 3rd Avenue, Minneapolis, MN 55414, USA*

[6]*Present address: Dept. of Geography and Geology, University of the West Indies, Mona Campus, Kingston 7, Jamaica*

Abstract: Submarine slides and debris flows are common and effective mechanisms of sediment transfer from continental shelves to deeper parts of ocean basins. They are particularly common along glaciated margins that have experienced high sediment flux to the shelf break during and after glacial maxima. During one single event, typically lasting for a few hours or less, enormous sediment volumes can be transported over distances of hundreds of kilometres, even on very gentle slopes. In order to understand the physics of these mass flows, the process is divided into a release phase, followed by break-up, flow and final deposition. Little is presently known regarding release and break-up, although some plausible explanations can be inferred from basic mechanics of granular materials. Once initiated, the flow of clay-rich or muddy sediments may be assumed to behave as a (non-Newtonian) Herschel-Bulkley fluid. Fluid dynamic concepts can then be applied to describe the flow provided the rheological properties of the material are known. Numerical modelling supports our assertion that the long runout distances observed for large volumes of sediments moving down gentle slopes can be explained by partial hydroplaning of the flowing mass. Hydroplaning might also explain the sharp decrease of the friction coefficient for submarine mass flows as a function of the released volume. The paper emphasizes the need for a better understanding of the physics of mass wasting in the submarine environment.

Introduction

Sediment mass-wasting in the form of slides, debris flows and turbidity currents on continental slopes represents an important process for transporting large volumes of sediments in the submarine environment. We use the term 'mass-wasting' in a broad sense to describe failure of a mass at the shelf break or on the upper slope, which subsequently starts to move downslope under the influence of gravity. Along the flow path, the mass may disintegrate and, depending on its rheology and external conditions, liquefy into a debris flow and also produce turbidity currents. Numerous subsea images of mass flows reveal a gradual transition from a typically blocky composition in the upper part to a more remoulded form in the middle and lower part of the mass flow (e.g. Booth *et al.* 1993).

Typically, large sediment volumes are involved in submarine mass-wasting, even on gentle slopes. A well-known example is the Storegga Slide, involving about 6000 km^3 of sediments, that took place on the Norwegian margin on a slope of about 1° or even less (Bugge *et al.* 1988). Of particular interest in the case of glacial margins are the often well defined mud-rich debris flows (up to 70% clay and silt) commonly associated with outlets of former large ice streams along the Eastern Canadian, East Greenland, Norwegian and Svalbard–Barents Sea margins (Aksu & Hiscott 1989, 1992; King *et al.* 1998; Dowdeswell *et al.* 1997; Solheim *et al.* 1998; Vorren *et al.* 1998).

From: DOWDESWELL, J. A. & Ó COFAIGH, C. (eds) 2002. *Glacier-Influenced Sedimentation on High-Latitude Continental Margins.* Geological Society, London, Special Publications, **203**, 73–87. 0305-8719/02/$15.00

The individual debris flows along the Norwegian and the Svalbard–Barents Sea margins involve volumes ranging from less than 1 to about 50 km^3 of sediments and cover areas of up to 2000 km^2 (Vorren *et al.* 1998).

A characteristic of submarine mass wasting is the long runout distance that, at times, can reach hundreds of kilometres. Information combined from glacially-influenced as well as non-glacial margins shows that the long runout distances (more than 100 km) generally occur on slopes of less than 2° (Booth *et al.* 1993; Vorren *et al.* 1998) and that the largest volumes of displaced sediments are associated with long runout distances (Fig. 1). Based on information from cable breaks, flow velocities in the range from 20 to 100 km hr^{-1} are calculated, even on slopes less than 1° (Heezen & Ewing 1952; Bjerrum 1971). The same data also show a tendency for the flow velocities to increase with the mobilized mass. Although the measured velocities may be those of the turbidity current in most cases, laboratory experiments (Mohrig *et al.* 1999) suggest that the dense debris flow may be even faster than the accompanying turbidity current, at least in the steeper parts of the flow path. Comparison with subaerial gravity mass flows (Simpson 1987) is difficult, given the steeper flow paths and smaller release masses typically encountered on land. Comparing the runout lengths of subaqueous and subaerial debris-flow events of similar release volume and drop height (Table 1), it appears that subaqueous debris flows are potentially more mobile than their subaerial counterparts, despite the reduced gravitational force and higher viscous drag in water. Understanding the dynamics of submarine mass flows thus represents a considerable challenge.

In this paper, we examine recent progress in modelling the muddy flows typical of high-latitude margins. We focus on the control exerted by the rheological properties of the material on processes that facilitate the long runout distances observed in debris flows on high-latitude margins, which may be applicable to submarine mass flows in general.

High-latitude debris flows: release mechanism and initial break up

Sediment release

Earthquakes are believed to be the most common cause of submarine landslides. Some directly documented landslides have taken place after major earthquakes. Examples include the Newfoundland slope failure following the 1929 Grand Banks earthquake (Heezen & Ewing 1952; Piper *et al.* 1999) and the catastrophic slides in Seward and Valdez, Alaska, associated with the major 1964 earthquake

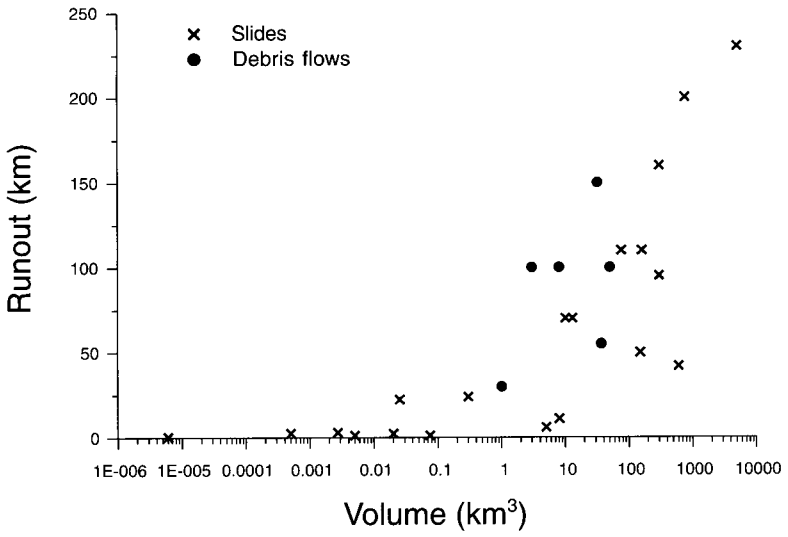

Fig. 1. Runout distances of submarine mass movements plotted against mobilized sediment volumes. Note the significant increase in run out as a function of volume when dealing with mass flows larger than 1 km^3. See Table 1 for data.

Table 1. *Characteristics of selected submarine slides including some data on subaerial slides*

Location	Slope angle (degrees)	Volume (km^3)	Runout L (km)	Height H (m)	H/L ratio	Reference
Submarine slides						
Grand Banks	3.5	$7.60x10^{1}$	110	365	0.00332	Prior & Coleman 1982
Hawaii	6.0		160	2000	0.0125	Prior & Coleman 1982
Kidnappers	2.5	$0.08x10^{-2}$	11	50	0.00455	Prior & Coleman 1982
Bay of Biscay			21	250	0.0119	Prior & Coleman 1982
Rockall	2.0	$3.00x10^{2}$	160	330	0.00206	Prior & Coleman 1982
Bassein	6.0		37	360	0.00973	Prior & Coleman 1982
Agulhas			106	375	0.00354	Prior & Coleman 1982
Copper River Delta	1.0		18	115	0.00639	Prior & Coleman 1982
Albatross Bank	7.0		5.3	300	0.0566	Prior & Coleman 1982
Portlock Bank	4.0		6.5	200	0.03077	Prior & Coleman 1982
Kayak Trough	1.0		15	115	0.00767	Prior & Coleman 1982
Magdalena	2.0	$0.30x10^{-2}$	24	1400	0.05833	Edgers & Karlsrud 1982
Valdez	6.0	$7.50x10^{-2}$	1.3	168	0.13125	Edgers & Karlsrud 1982
Mississippi River Delta	0.5	$4.00x10^{-2}$		20		Edgers & Karlsrud 1982
Suva	3.0	$1.50x10^{-1}$		100		Edgers & Karlsrud 1982
Sagami Wan	11.0	$0.70x10^{2}$				Edgers & Karlsrud 1982
Scripps Canyon	7.0	$5.00x10^{-5}$		6		Edgers & Karlsrud 1982
Orkadalsfjord		$2.50x10^{-2}$	22.5	500	0.02222	Edgers & Karlsrud 1982
Sandnesjoen		$5.00x10^{-3}$	1.2	180	0.15	Edgers & Karlsrud 1982
Sokkelvik		$5.00x10^{-4}$	2.5	120	0.048	Edgers & Karlsrud 1982
Helsinki		$6.00x10^{-6}$	0.4	11	0.0275	Edgers & Karlsrud 1982
Storegga 1		$5.50x10^{3}$	400	1700	0.00425	Bugge *et al.* 1988
Storegga 2		$5.50x10^{3}$	850	1700	0.002	Bugge *et al.* 1988
Trænadjupet	1.25	$7.60x10^{2}$	200	250	0.00125	Laberg & Vorren 2000
Cape Fear	4.2		30	700	0.02333	Poponoe *et al.* 1993
Blake Escarpment	8.6	$6.00x10^{2}$	42	3600	0.08571	Dillon *et al.* 1993
East Break East	1.5	$0.13x10^{2}$	70	1150	0.01643	McGregor *et al.* 1993
East Break West	1.5	$1.60x10^{2}$	110	1100	0.01	McGregor *et al.* 1993
Navarin Canyon	3.0	$0.05x10^{2}$	6	175	0.02917	Carlson *et al.* 1993
Seward		$2.70x10^{-3}$	3	200	0.06667	Hampton *et al.* 1993
Alsek	1.3		2	20	0.01	Schwab & Lee 1993
Sur	0.5	$0.10x10^{2}$	70	750	0.01071	Gutmacher & Normark 1993
Santa Barbara	4.8	$2.00x10^{-2}$	2.3	120	0.05217	Edwards *et al.* 1993
Alika 2		$3.00x10^{2}$	95	4800	0.05053	Normark *et al.* 1993
Nuuanu		$5.00x10^{3}$	230	5000	0.02174	Normark *et al.* 1993
Tristan de Cunha		$1.50x10^{2}$	50	3750	0.075	Holocomb & Searle 1991
Debris flows						
Isfjorden	3.5	$0.01x10^{-2}$	30	1830	0.061	Fossen 1996
Storfjorden	1.5	$0.08x10^{-2}$	100	2000	0.02	Laberg & Vorren 1995
Bear Island	0.6	$0.32x10^{2}$	150	1600	0.01067	Vorren *et al.* 1998
North Sea	0.7	$0.50x10^{2}$	100	750	0.0075	King *et al.* 1996
Newfoundland	0.75	$0.03x10^{-2}$	100	1700	0.017	Aksu & Hiscott 1992
Baffin Bay	1.8	$0.037x10^{-2}$	55	1000	0.01818	Aksu & Hiscott 1989
Subaerial slides						
Mount Rainier		$1.00x10^{0}$	120	4800	0.04	Vallance & Scott 1997
Nevados Huascaran		$1.00x10^{-1}$	120	6000	0.05	Plafker & Ericksen 1978
Nevado del Ruiz		$1.00x10^{-2}$	103	5190	0.05039	Pierson *et al.* 1990
Mount St. Helens		$1.00X10^{-2}$	44	2350	0.05341	Fairchild & Wigmosta 1983
Mount St. Helens 2		$1.00X10^{-2}$	31	2150	0.06935	Pierson 1985
Wrightwood		$1.00X10^{-3}$	24	1524	0.0635	Sharp & Nobles 1953
Mount Thomas		$1.00x10^{-4}$	3.5	600	0.17143	Pierson 1980
Wrightwood 2		$1.00x10^{-4}$	2.7	680	0.25185	Morton & Campbell 1974
Santa Cruz		$1.00x10^{-4}$	0.6	200	0.33333	Wieckzorek *et al.* 1988

(Coulter & Migliaccio 1966; Lemke 1967). Cyclic loading by storm-wave action and expansion of gas hydrates are the other commonly cited causes (Kvenvolden 1994; Kvalstad *et al.* 2001). In all these cases, failure of sediments is caused by instability induced by an external mechanism or event and a failure plane can normally be recognized.

However, in the case of glaciated continental margins, an external trigger may not be required. High sedimentation rates have been recognized as a potential mechanism for failure (e.g. Vorren *et al.* 1998; Dimakis *et al.* 2000). On glacial margins, where high sedimentation rates are the norm rather than the exception, the depositional environment itself could be an inherently unstable system: the sediments fail when the rate of sedimentation exceeds some threshold value, depending on factors such as the rheology of the sediments, the mechanism of sediment transport, and the bed slope. This may be true particularly in cases where fast-flowing ice streams deliver sediments with a high clay content to the upper slope in the form of deformation till, as opposed to delta-fed deep-sea fans where the sediments are first suspended in water upon delivery before settling out. Sediment supply in the form of deformation till, as is interpreted to be the case for northern North Atlantic margins, favours under-consolidation and rapid build-up of excess pore pressure, eventually leading to failure.

For the deposits off Bear Island and Storfjorden, average sedimentation rates during glacial periods are estimated to be in the range of tens of centimetres per year (Laberg & Vorren 1995). For the Bear Island Fan, Dimakis *et al.* (2000) showed that the build-up of excess pore pressure due to rapid sedimentation rates under glacial advance could lead to failures on the upper continental slope. By using an infinite slope stability analysis together with excess pore pressure, Dimakis *et al.* (2000) argued that the observed uniformly thick, layered slope deposits seen on the Bear Island Fan can be explained through a regenerative process. In this process, glacially-derived sediments accumulate over a source area until they become unstable through build-up of excess pore pressure. A minimum sedimentation rate of 20 cm a^{-1} is found to be required for excess pore pressure to build up in this case. Failure takes place along a plane within the accumulated sediment mass such that the sediments above the plane move downslope without generating any slide scars, while the sediments below it remain and become the new surface for sediment deposition (Dimakis *et al.* 2000). The cycle is repeated whenever the sediment mass becomes thick enough to exceed the failure criteria. Failures are calculated to occur after 95–170 years of high-rate sedimentation and to remove 25–30% of the sediments deposited during the period. The analysis also shows that an increase in slope will cause more frequent but smaller failures. This may also explain why larger volumes of sediments are mobilized on gentler slopes.

Although the model of Dimakis *et al.* (2000) was presented for a glaciated margin during periods of glacial expansion, it may also be valid in typical delta environments where the combination of sedimentation rate and sediment composition (high clay content) leads to periodical build-up of sufficient excess pore pressure so as to cause instability and failure.

Initial break-up

The debris flows recorded on high-latitude margins do not show the presence of any slide scars but rather a well-defined flow mass all the way along the slope (e.g. Vorren *et al.* 1998). The flow often forms characteristic elongated bodies running all the way from the upper to the lower slope. This suggests liquefaction immediately following failure. Thus, although soil-mechanical parameters define the state of sediments on the upper slope, the behaviour of the moving mass in the mid- and lower-slope regions is better explained by principles of fluid flow regardless of initial processes (Fig. 2). Failure and the initial break-up are only discussed briefly here. It is the mid- and lower-slope processes that we attempt to describe in detail.

After the release of a debris flow, the flow dynamics will depend on evolving properties of the flowing sediment such as granulometry, yield strength, viscosity, and pore fluid pressure. Little is known about the progression of the break-up and the early phase of flow. Theoretical considerations suggest that a wide variety of scenarios may occur in different slide events depending on grain size, degree of consolidation and strength/intensity of the initiating mechanism. For example, in strongly underconsolidated, homogeneous soils subject to a powerful earthquake, liquefaction may occur almost instantaneously throughout most of the released mass because the jolt from the earthquake propagates through the soil and is strong enough to break its weak texture. If the soil has a high content of fines, a debris flow with only relatively small clasts is expected to result, whose properties approach those of a mudflow. Conversely, significant small-scale variations of

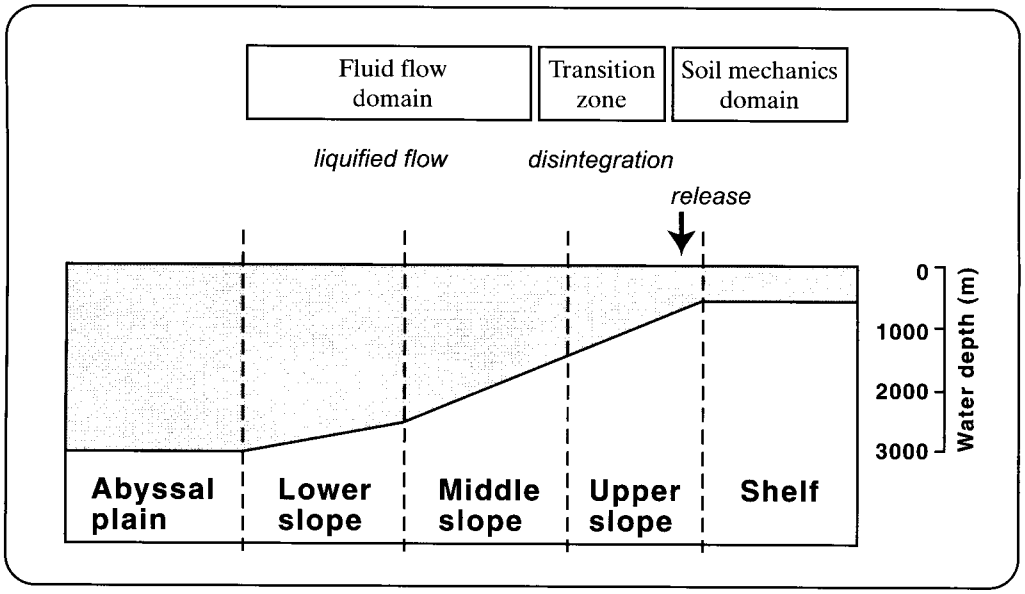

Fig. 2. The various stages of sediment mass behaviour along the flow avenue, starting as a block (soil mechanics domain) and gradually being transformed in a liquefied flow characterized by fluid dynamics.

soil properties will lead to a form of debris flow with a large fraction of clasts up to boulder size.

If distinct layers exist in slightly underconsolidated or normally-consolidated sediment, a situation may occur where the seismic waves are too weak to break the inter-particle bonds in the bulk of the soil, but shear fractures are generated along the weakest layers. Where the weak layer collapses, it can no longer support the shear stresses generated by the overlying slab. At the circumference of the collapsed area, the shear stresses are significantly increased and drive fracture propagation along the weak layer. The slab is released when the downslope gravitational force on the slab above the collapsed part of the weak layer exceeds the tensile, shear and compressive forces that the surrounding area can exert on the slab to hold it in place. The gravitational force grows with the collapsed area, but the resistive forces increase only with its circumference. Note also that the maximum size of the slab grows with its strength and diminishes with increasing slope angle. This scenario indicates that huge slabs of intact soil might be released instantaneously under certain conditions; it is closely analogous to the release mechanism of snow-slab avalanches (e.g. McClung & Schaerer 1993, for an introduction). Two notable differences should be pointed out, however. In subaqueous landslides, the triggering earthquake is effective in a large area and excess pore pressure in the weak layer plays a crucial role, whereas it is of little importance in snow avalanche release.

The work required for breaking up a large slab ultimately comes from gravitational energy released when the slab moves down the incline. The central question is whether this work is a large fraction of the total initial potential energy. In the case of brittle tensile fracture, the work required for breaking a slab of volume V and tensile strength σ_t into two halves is $W_h = V\sigma_t^2 / (2E)$, assuming the elastic energy to be completely dissipated after fracture. Here, E is Young's modulus, and we consider a block of length l, width w and height h. As the slab is stretched to failure along l, at stress σ_t, its length increases by $\Delta l = l \times \sigma_t / E$. The mechanical work is $\sigma_t \times \Delta l \times w \times h / 2 = V\sigma_t^2 / (2E)$, as indicated above. The same result is obtained for fracture in the two other directions.

Dividing a one-dimensional object of length l by cutting n times in the middle of each newly-formed piece, one obtains a total of 2^n pieces of length d, namely, $n = \log_2(l / d)$. Extending the reasoning to three dimensions, if the break-up mechanisms were to break each block repeatedly into two parts of equal size, a total of $n = \log_2(l / d) + \log_2(w / d) + \log_2(h / d) = \log_2(V / V_p)$ fracture sequences involving all

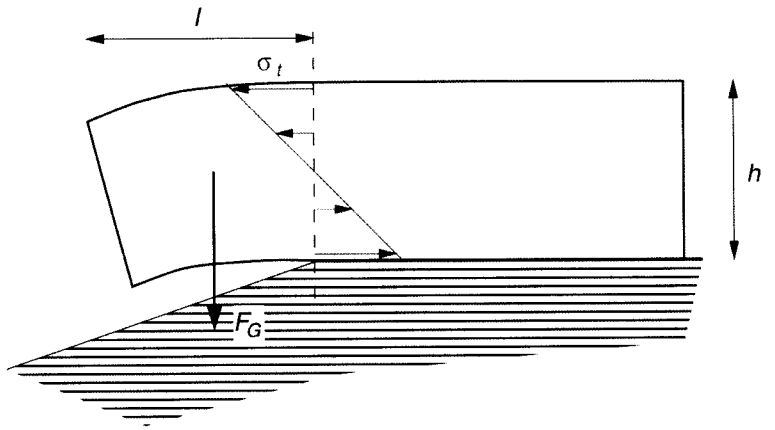

Fig. 3. Simplified model for the effect of sea-floor undulations found, for example, below the Storegga Slide headwall. Tensile and compressional stresses in a large flowing slab encountering an abrupt slope change.

particles and total work $W_{total} \approx W_h \times \log_2 (V / V_p)$ would be required to reduce a slab of volume V to particles of volume $V_p = d^3$. Alternatively, if mostly single particles were chipped off the slab by collisions, the total work would be $W_{total} \approx W_1 \times V / V_p$, with W_1 the average binding energy of a surface particle. Lacking a detailed model for calculating W_1 at present, we expect it to be proportional to the volume affected by the collision-induced deformation, which should be somewhat larger than V_p, and the square of the (shear) strength $\sigma_s > \sigma_t$. The total break-up work is then similar in order of magnitude to the first case. For Young's modulus $E \geq 10^7$ Pa and tensile strength $\sigma_t \approx 10^5$ Pa, typical of submarine sediments, a drop of only 3 m releases gravitational energy equal or larger than the work needed to break a slab of 1 km^3 into particles of 1 mm^3. Despite the large uncertainties in such estimates, we tentatively conclude that the break-up rate is not so much limited by the energy supply as by the efficiency of the various processes that contribute to break-up.

One such break-up process may be due to ocean-bed undulations which are found, for example, in bathymetric data from slide areas such as Storegga (P. Bryn pers. comm.), with amplitudes of several tens of metres at length scales of 0.1 to 1 km. The curvature radius is then not much larger than the slab height. Large tensile and compressive stresses are induced in a sediment slab sliding over such terrain. For a crude estimate, we equate the gravitational torque from the part of a slab protruding over the crest of an undulation to the torque created by the tensile and compressive stresses in a cross-section of the slab as in elementary beam theory (Fig. 3). Assuming a tensile strength of about 100 kPa and a slab height of 100 m, we find that pieces about 10–30 m long should break off at the front of the slab. Where such bed undulations are present, this appears to be a rather effective first-stage break-up mechanism. It is accompanied by strong agitation of the fragments, facilitating remoulding and incorporation of water.

At a later stage, collisions between blocks may be the driving break-up mechanism. The processes involved are quite complex and presumably depend strongly on a number of parameters, among them the soil properties, the fines content that strongly influences the viscosity of the pore fluid, and the velocity, size and shape distributions of the fragments. Of importance here, and as yet poorly constrained, is the role of interstitial fluid (Iverson 1997). Its presence on the one hand dampens velocity fluctuations and on the other hand increases the mobility of the flowing material and the velocity gradients which, in turn, drive the generation of disordered motion of particles (granular temperature). More detailed investigation of this subtle interplay between particles and interstitial fluid will be important not only for describing the break-up process, but also for modelling velocities, runout distances and deposits.

To summarize, depending on the soil properties and the external triggering mechanism, the initial slab may liquefy quasi-instantaneously or undergo a more gradual transition from large

blocks to a more fine-grained composition. The duration of the transition may vary from a small fraction to all of the flow duration. Present knowledge of the possible scenarios, the conditions of their occurrence, and their dynamics is still very rudimentary.

High-latitude debris flows: flow dynamics and flow simulations

Flow models

Presently, two classes of model are widely used to simulate subaqueous mass flows, namely visco-plastic models (e.g. Johnson 1970; Huang & Garcia 1998, 1999) and granular models (Savage & Hutter 1989) incorporating the effects of viscous pore fluid (Iverson 1997) as well as Bagnold's dispersive pressure caused by grain–grain and grain–fluid interaction (Norem *et al.* 1987). Both types of model have been discussed widely (Norem *et al.* 1990; Hampton *et al.* 1996; Locat & Lee 2001; Iverson 1997; Iverson & Vallance 2001), the latter mostly with a view towards terrestrial debris flows characterized by a very low content of fines (less than 5% silt and clay). The visco-plastic models, on the other hand, have been developed for clay-rich or muddy materials with cohesion and a very low content of coarse particles capable of particle–particle interactions, a situation outside the range of applicability of a true granular flow model.

Grain size distribution in the debris flow deposits along the North Atlantic margins is influenced strongly by the input of fine-grained glacial erosion products. Typical particle distribution for the debris flows and other mass displacements is 30–40% clay, 30–40% silt and 20–30% sand (Vorren *et al.* 1998). Gravel is almost missing. Due to this almost complete lack of particles large enough for particle–particle interaction and the high clay content, we are inclined to favour the visco-plastic model for explaining debris-flow dynamics along these margins. Recent modelling of muddy debris flows using the visco-plastic approach shows a high degree of correspondence between observed and modelled runout distances for small debris flows (Huang & Garcia 1999). The sediment composition in modelling by Mohrig *et al.* (1998, 1999) was selected to reflect field data, supporting our choice for muddy, almost clast-free debris flows.

In its simplest form, visco-plastic behaviour can be described by the so-called Bingham rheology where the stress τ and strain $\partial U/\partial y$ (where U is the velocity component parallel to the bed and y is the co-ordinate perpendicular to it) are linearly related as follows:

$$|\tau| = \tau_y + \mu_B \left|\frac{\partial U}{\partial y}\right|^n \quad \text{for } |\tau| \geq \tau_y, n = 1$$

where τ_y is the yield stress and μ_B the dynamical Bingham viscosity. The stress–strain relation for a Bingham fluid in laminar flow implies that no deformation takes place until a specified yield stress is applied to the material, after which the deformation is driven by the excess stress beyond this yield stress. The visco-plastic rheological relation dictates the division of the flow into a plug layer on top of a shear layer.

More general relations such as a Herschel-Bulkley rheology, where the stress depends non-linearly on the strain rate (exponent $n > 0$ instead of $n = 1$ in the equation above), and a bi-viscous rheology (which reduces to a Newtonian flow for small shear rates and a Bingham fluid for high shear rates: Locat 1997) have also been proposed. These constitutive relations provide a more general rheological behaviour. For $0 < n < 1$, the Herschel-Bulkley rheology describes shear thinning, namely the observed tendency of yielded mud to become less viscous with increasing shear rate. Both the Herschel-Bulkley and the bi-viscous rheologies have been implemented in particular in the BING code (Imran *et al.* 2001). However, experiments on materials with high clay content (about 40% clay, 40% silt and 20% sand) reveal an exponent n very close to unity (Huang & Garcia 1999). Since this is the kind of material we consider in our study, we make use of a simple $n = 1$ Bingham fluid. Considering the uncertainties in the rheology of submarine mass flows, many of which have variable compositions, a Bingham rheology is suitable as a first-order approximation of the flow. In addition, it will be shown that hydroplaning (see below) is not strongly dependent on the rheology of the sediment, provided the characteristic critical velocity is attainable.

A related problem concerns the variation of pore water pressure during the flow. In what follows we do not explicitly consider excess pore pressure, but more appropriate models, especially for sandy debris flow, should incorporate the generation and diffusion of excess pore pressure as a dynamic process that influences the rheology of the material. We assume that the very low permeability of clay-rich sediment hinders efficient diffusion of excess pressure through the moving mass, at least during the relevant time scale of a few hours. The chosen

yield stress and Bingham viscosity are to be interpreted as mean values over the flow episode.

Flow models: hydroplaning

Recent studies have shown that the classical visco-plastic concept, too, falls short of fully simulating the long runout distances for subaqueous debris flows, at laboratory scale as well as for the debris flows observed on the Svalbard–Barents Sea margin (Huang & Garcia 1999; Marr *et al.* 2002). In recent years, hydroplaning has been suggested as a possible mechanism for debris flows covering long distances on low-angle slopes (Mohrig *et al.* 1998, 1999; Harbitz *et al.* 2001). Hydroplaning is shown to occur in a cohesive mass once that mass exceeds a critical velocity such that the flow cannot displace the ambient fluid fast enough. As a result, the head of the flow is lifted and a water layer intrudes beneath the moving mass. The intruding water layer acts as a lubricant, reducing basal friction and increasing head velocity. Although some mud may be mixed into the thin water layer, increasing its viscosity, the resulting slurry will still have a significantly lower viscosity than the mud.

The concept of hydroplaning is of particular interest since it produces large runout distances even at relatively high yield stresses. As the water film greatly reduces the basal shear stress, rapid flow without or with negligible erosion of the underlying strata can be explained quite naturally. Although hydroplaning has been observed directly only in the laboratory so far, the same effect must occur in nature as well. At the heart of the phenomenon is the balance between the pressure in the basal water layer, characterized by the stagnation pressure $\rho_w U^2 / 2$, and the overburden load of the mud layer, $(\rho_d - \rho_w) g H$, where ρ_d and ρ_w are the mud and water densities, respectively. The dimensionless ratio of these pressures is, up to a factor of 2, the square of the densimetric Froude number. In going from the laboratory to the field scale one can use distorting modelling relations between the physical and geometrical quantities. The appropriate scaling factors can be obtained, in principle, by keeping the same value for the relevant dimensionless numbers, like the Froude and the Reynolds numbers. It has been shown that present experiments are well scaled except for the dimensions of the microstructure: that is, the grain size (G. Parker pers. comm). Focusing on the rheological properties of the sediment (viscosity and yield strength) rather than the grain size circumvents the problem of scaling the microstructure. Through scaling down the values of viscosity and yield strength and scaling up the slope of the experimental facility, it is possible to model field scale debris flows in the laboratory. Thus, although the scaling problem is still under investigation, we believe that a direct application of the experimental results to natural debris flows is appropriate.

Other explanations for high mobility of compacted sediments have been put forward recently by Gee *et al.* (1999). Making specific reference to the Saharian debris flow, which is composed of two different layers, a volcaniclastic layer overlain by pelagic mud, these authors proposed that long runouts are attained due to an increase of pore water in the volcaniclastic sediments by overloading from the muddy layer. Although the model of Gee *et al.* (1999) might be applied to this specific case, in view of the relative commonness of long run-out distances of subaqueous debris flows, we believe that a more general process is likely to be at work.

For a closer look at the effects of hydroplaning, the BING program, describing the movement of non-hydroplaning flow (Imran *et al.* 2001), was modified to include a water layer at the bottom of the moving sediment mass (Water-BING). Hydroplaning starts when the velocity at the front of the flow is sufficiently high for the water to lift the moving mass. Subsequent evolution of the water layer is calculated numerically from the vertically-integrated Navier-Stokes and continuity equations for the water layer and appropriate boundary conditions. Hydroplaning is invoked once the water thickness becomes larger than a minimal thickness representing the size of the bed and sediment irregularities.

When the mud or debris is hydroplaning, the stress at the boundary with the basal water layer is approximately $\mu_w U / D_w$, where U is the velocity of the hydroplaning slab, D_w is the thickness of the water layer and μ_w is the water viscosity. Using values of the order of $U \approx 10$ m s^{-1}, $\mu_w \approx 0.005$–0.01 kg m^{-1} s^{-1} and $D_w \approx 1$ cm, one finds a shear stress between 5 and 10 Pa, a value which is much smaller than the yield stress of the sediment, $\tau_y \approx 8$–15 kPa. The hydroplaning mass thus moves rigidly on top of the water layer, essentially without shearing.

To understand the forces at work as the sediment is moving, we can imagine dividing the flowing material into vertical elements, the positions of which change in time. If the material is hydroplaning, the bed-parallel forces acting on a slice of sediment are: 1) the

component of the gravity force parallel to the bed; 2) the earth pressure gradient; a force arising from variations in the height of the material and directed from thick toward thin sediment; 3) the internal resistance force of the material, determined by both the yield stress and viscosity; 4) the drag force due to the interaction of the moving mass with embedding water. The equation of motion for a hydroplaning gravity flow can be written simply from Newton's law as

$$\frac{dU}{dt} = -\frac{\rho_d - \rho_w}{\rho_d} - \frac{\partial}{\partial x}(D + D_w)\, g_y - \frac{\tau_w}{D\rho_d} + \frac{\rho_d - \rho_w}{\rho_d} g_x - f_{drag}$$

where the co-ordinate x denotes the distance along the flow, U is the velocity of an element of flowing sediment, D is the local sediment thickness, ρ_d and ρ_w are the sediment and water densities, respectively, g_x and g_y are the components of the gravity acceleration parallel and perpendicular to the bed, respectively, f_{drag} is the specific drag force due to the resistance of the water on top of the flowing mass and τ_w is the frictional stress between the sediment and the water below. The specific drag force can be written as

$$f_{drag} = \frac{1}{2} U^2 \frac{\rho_w}{\rho_d D}\left[C_F + \left|\frac{\partial D}{\partial x}\right| C_P\right]$$

where C_F and C_P are the frictional and pressure drag coefficients, respectively. The value of these constants can be estimated from flow experiments against bodies of given shape at fixed Reynolds number. At Reynolds numbers of the order 10^7–10^9, we estimate from standard tables (Newman 1977) values of about C_F = 0.003 and C_P = 0.01 or smaller. It is possible that higher pressure drag coefficients should be used for well-developed sediment heads. However, due to the pronounced flatness of the sediment, an arbitrary increase in the value of the pressure drag coefficient C_P does not produce significant changes. The roughness of the solid material at the interface with the liquid might change the effective value of drag coefficients (Schlichting 1968). The space derivative results from the calculation of the total sediment surface directed perpendicular to the ambient water velocity. One should keep in mind that our approximation for the drag force is rather crude. We are not aware of any complete model for the drag force in this problem. Furthermore, the interaction of the sediment with ambient water generates a region of the size of the boundary layer where water is in a turbulent regime. The strong mixing with mud, which might later produce a turbidity current, changes locally and unpredictably the properties of both the water and the flowing sediment. In addition, a shear region exists in the sediment due to the shearing effect induced by the drag whereas, in calculating the equations of motion, we considered the sediment as a rigid body.

In the case of non-hydroplaning, the rigid 'plug' layer is coupled with a shear layer below, the flow being determined by the rheological properties of the material. As a result, the resistance is in general substantially increased. The complete equations for the shear flow can be found in Huang & Garcia (1998) and Imran *et al.* (2001). When hydroplaning takes place, the frictional stress between the sediment and the bottom is sensitive to the properties of the water layer rather than to the rheology of the sediment. In order to calculate the stress between the mud and the water, one needs to solve the mass and momentum equations in the water layer as a function of time.

Modelling results

In the following, we briefly present results from numerical simulations of a mass flow obtained with the BING code (without hydroplaning) and the modified version Water-BING that includes hydroplaning. The initial configuration consists of a 20 km wide and 300 m thick deposit lying on a less than 1° slope, from the position x = –20 km to x = 0. Starting from rest, the sediment accelerates and within ten minutes reaches velocities of 36 m s^{-1} and 60 m s^{-1} without and with hydroplaning, respectively. Note that a substantial contribution to the acceleration at the beginning of the flow comes from the earth pressure gradient. The material properties used in the simulation are taken from Elverhøi *et al.* (1997) and Marr *et al.* (2002): density ρ_d = 1800 kg m^{-3}, viscosity μ_B = 300 Pa s and yield stress τ_y = 15 kPa.

To estimate the yield stress of a debris flow at rest one can use the concept that a viscoplastic fluid on a slope φ will stay at rest if the shear stress, $\Delta\rho\, g\, D \sin\varphi$, where $\Delta\rho$ is the density difference between the sediment and water and D is the thickness, is equal or smaller than the yield stress, τ_y (Johnson 1970). This leads to a direct relation between sediment thickness and yield stress, $D = \tau_y / (\Delta\rho\, g \sin\varphi)$. Without hydroplaning, the mass covers about 25 km before coming to rest, whereas the hydroplaning mass continues to flow (Fig. 4a). The

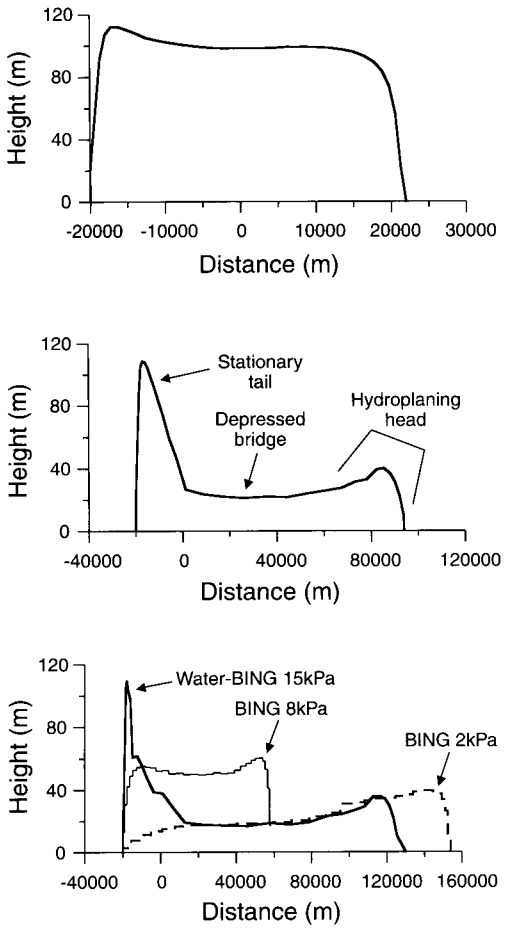

Fig. 4. (**a**) Simulation of non-hydroplaning debris flow using BING. Final geometry of the deposit after 25 minutes of run-time is shown. Sediment properties: density, ρ_d = 1800 kg m^{-3}; viscosity, μ = 300 Pa s; and yield stress, τ_y = 15 kPa. (Data from Elverhøi *et al.* 1997; Marr *et al.* 2002). (**b**) Simulation of hydroplaning debris flows using Water-BING. Sediment properties as in (a). Run-time 32 minutes. (**c**) Comparison of final deposits after the completion of hydroplaning and non-hydroplaning simulation runs. For the non-hydroplaning case, the yield strength has to be reduced by one order of magnitude to achieve the same runout distance as the hydroplaning case.

non-hydroplaning mass stops essentially because the sediment thickness has become too small to maintain a shear layer. On the other hand, the hydroplaning sediments continue flowing as, in this case, the flow is determined by the physical conditions of the water layer rather than the rheological properties of the sediments. The hydroplaning flow comes to rest at 130 km (Fig. 4c), which is closer to the runout length observed for the debris flows on the western Barents Sea continental margin (Elverhøi *et al.* 1997).

The numerical simulations also reveal that sediments undergo non-uniform acceleration during the flow. Water intrudes from the head of the mass and then migrates under the main body of the sediment. The front of the flow begins to hydroplane earlier and moves forward; the main body accelerates moderately while the tail remains stationary. The head of the deposit tends to be detached from the rest of the body. This concurs with the results of small-scale laboratory experiments (Mohrig *et al.* 1999).

The numerical simulations also demonstrate the effects of variations in yield strength and viscosity on the flow (Fig. 4c). In the absence of hydroplaning, yield stress has to be reduced by one order of magnitude (to 2 kPa) in order to reproduce the distances reached by hydroplaning sediments. Such low values are unrealistic for such clay-rich sediments and would not allow deposits of the thickness commonly observed along the Norwegian continental slope (Marr *et al.* 2002).

Runout distances with and without hydroplaning are shown as functions of yield strength (Fig. 5). The reason for the dependence of hydroplaning flow on the yield strength, as seen from the figure, is that the critical velocity is reached early with small yield stresses, causing hydroplaning to start early. As shown by experimental studies (Mohrig *et al.* 1999) hydroplaning sediment can be treated as a rigid block flowing in a low-viscosity medium exerting drag forces. Once initiated, hydroplaning flow is controlled by the behaviour of the ambient water and is independent of the sediment rheology. Thus, simulations confirm that hydroplaning flows cover much longer runout distances than non-hydroplaning flows, as has been observed earlier in laboratory experiments (Mohrig *et al.* 1999).

The value of viscosity is more uncertain, because it is not constrained strongly by the height of the final deposit. However, in the presence of high yield stress, the flow is insensitive to viscosity. In the simulated runs, a decrease of the viscosity by one order of magnitude increases the total runout distance by only 8%. Even decreasing the viscosity unrealistically by four orders of magnitude does not change this conclusion. The results concur with Locat & Lee (2001), who concluded that the contribution of yield strength to flow resistance is three orders of magnitude larger than

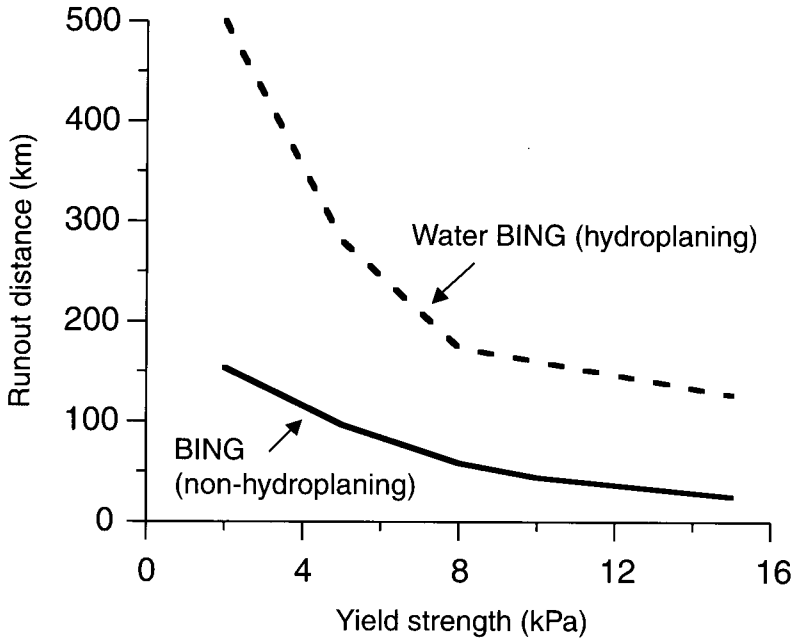

Fig. 5. Plot showing the run-out distances with and without hydroplaning as a function of sediment yield stress.

viscosity. Therefore, a small value of the viscosity does not seem to be the cause of the large runout distance of debris flows on low-angle slopes.

The results of our simulations depend on a set of parameters and initial conditions, some of which are not well-known in nature. When the water penetrates below the mass flow, it mixes with the sediments to form a slurry with different rheological properties. The Water-BING model accounts for this by attributing a viscosity value to the water that is ten to twenty times larger than the viscosity of pure liquid (Mohrig *et al.* 1998). In addition, water residing under the sediment for a long time will become completely mixed with it, a process made more effective by the turbulence in the water layer. This effect, which is not incorporated in our model, may eventually bring hydroplaning to an end. Water penetration through the debris is possible, but very limited if the material is mostly composed of clay, with permeability probably as low as 10^{-6} cm s^{-1}. This quantity might be substantially higher in debris flows with more sandy composition. This is one of the reasons why sandy debris flows do not hydroplane in the laboratory and are dominated by the effect of pore water pressure diffusion through the bulk sediment.

Our model presents some uncertainties associated with the initial water profile, the front and surface drag force and especially the initial size and shape of the sediment slab. The larger the initial height, the higher are the velocities and the runout distances. The dynamical problem is thus connected closely to the still problematic question of the triggering mechanism discussed earlier.

Mobility and runout of submarine mass wasting: discussion and concluding remarks

One of the main challenges in studies of submarine mass-wasting is to explain the high mobility of debris flows. The fundamental process with regard to the mobility of submarine sediments is the transformation of potential energy of the sediment mass into work required to, firstly, dislocate (break-up) and, subsequently, to move the displaced block downslope while overcoming the various resistances (e.g. friction, drag). The displacement of the centre of mass of a debris flow is characterized by the horizontal distance L from source to deposit and the vertical elevation of the debris flow source above the deposit, H.

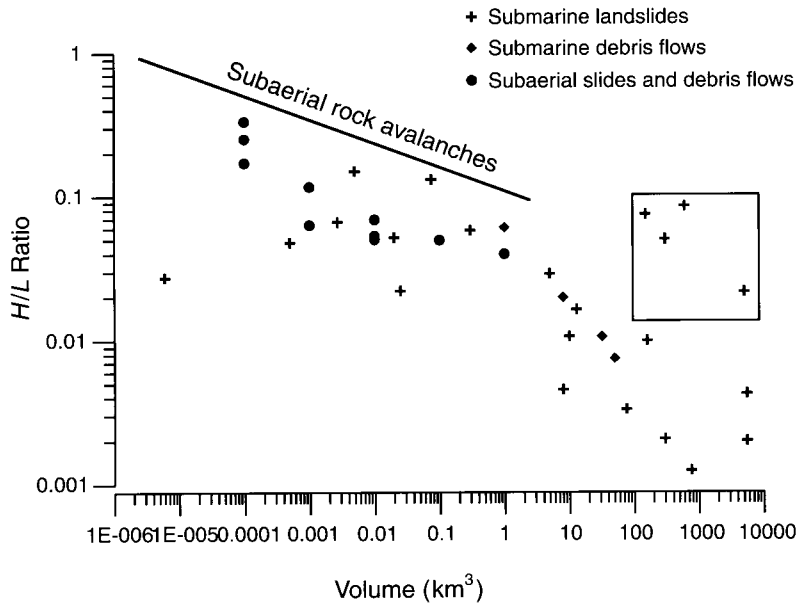

Fig. 6. Mobility of submarine mass flows, expressed as *H/L* ratio plotted against sediment volume (for data see Table 1). Data for selected subaerial slides/debris flows are also included (source: Iverson, 1997). Data points in the rectangle represent submarine volcanic debris and carbonate rock falls, for details see text.

Defining the effective friction coefficient, f, by the relation $f = H/L \tan \beta$ where β is the average slope angle from the release zone to the deposit (Scheidegger 1973), one readily obtains $f = \tan \phi$ if only Coulombian (dry) friction is present — the effective friction coefficient is equal to the tangent of the bed friction angle ϕ for granular material. Since ϕ is an intrinsic property of a granular material and the bed, this relationship implies that the net efficiency (or mobility) of a debris flow is independent of the mass involved. Observations, however, show a clear increase of the net efficiency (or decrease of the effective friction) with increasing mobilized mass. Iverson (1997) argued that, although not yet clearly understood, the increase in mobility with increasing volume may be attributed largely to changes in sediment composition and rheology. Edgers & Karlsrud (1981) developed a simple flow analysis to estimate the runout velocities of submarine slides. They used data from five submarine slides to back-calculate the equivalent sediment viscosities and compared these values with estimates of equivalent viscosity in subaerial quick clay slides back-calculated in a similar way. Good correspondence between the two viscosity estimates led them to conclude that viscous flow was an important mechanism in submarine slides just as in the case of quick clay slides. However, Edgers & Karlsrud's model does not incorporate yield strength. As shown by this work, yield strength is a much more significant parameter than viscosity in determining flow behaviour of debris flows. The Edgers & Karlsrud model, therefore, is not adequate for analysing the mobility of submarine mass-wasting.

The ratio of *H/L* and volume for different mass flows is shown in Figure 6. It includes slides, debris flows and rock avalanches from different parts of the world, both in submarine and in subaerial environments. Submarine slides smaller than about 1 km^3 all have ratios larger than 0.02. The same value represents instead an *upper* limit when the volume is larger than 1 km^3. The exceptions, marked in the figure by a rectangle, are primarily debris *avalanches* containing both sediments and rock fragments that could be as large as 1 km in the horizontal direction (Normark *at al.* 1993). The other outlier represents limestone blocks, up to 10 km across and bounded by faults, that fall off when carbonate cliffs become oversteepened due to erosion (Dillon *et al.* 1993). These outliers, thus, do not represent the muddy mass flows considered in the present study. Interestingly, they fall on the continuation of the line for subaerial rock avalanches (Scheidegger 1973), indicating a similarity of processes between subaerial and submarine rock avalanches. For

slides and debris flows, the critical volume of 1 km^3 marks a change in the dynamic behaviour of the flow, as can be seen from the steepening of the curve. For volumes above1 km^3, a fit to the available data indicates H/L to be proportional to $V^{-0.34}$ and to decay both much more rapidly than below the 1 km^3 limit, and also more rapidly than for rock avalanches. We suggest that for volumes smaller than 1 km^3, the flow is controlled primarily by the rheology of the moving mass. When the volume exceeds this value, the flow is associated with an increase in the velocity beyond the critical value required to initiate hydroplaning. Once the mass begins to hydroplane, its mobility becomes independent of the rheology. Note that this conclusion is based on the analysis of a limited number of data points. It will be interesting to see if this view can be maintained as more data become available.

We have examined some of the problems regarding the initiation phase and dynamic behaviour of submarine mass flows, particularly in relation to glacier-influenced continental margins. For clay-rich sediments which do not reach the critical velocity for hydroplaning, the visco-plastic model appears to be suitable for describing the flow in terms of fluid dynamics of a non-Newtonian fluid. This study indicates that large mass flows (larger than 1 km^3 in volume) might reach a sufficient velocity to initiate hydroplaning. This would explain the long runout distances reached on gentle slopes, without assigning unreasonably small values for yield strength, and the steep decrease of the H/L ratio as a function of the volume. On the other hand, for small slides and debris flows, covering short distances, a visco-plastic model without hydroplaning is well suited. In this case the flow behaviour is determined by the sediment rheology.

The work presented in this paper was carried out as part of projects funded by the EU (COSTA project no. EVK3-CT-1999-0006), VISTA (project 6241) and the Norwegian Research Council (NFR project 1333975/431). The authors wish to thank R. Hiscott and P. Talling for their careful and extensive reviews of the manuscript, which helped to improve the paper considerably.

References

AKSU, A. E. & HISCOTT, R. N. 1989. Sides and debris flows on the high-latitude continental slopes of Baffin Bay. *Geology*, **17**, 885–888.

AKSU, A. E. & HISCOTT, R. N. 1992. Shingled Quaternary debris flow lenses on the north-east Newfoundland Slope. *Sedimentology*, **39**, 193–206.

BJERRUM, L. 1971. *Subaqueous slope failures in Norwegian fjords*. Norwegian Geotechnical Institute, **88**, 1–8.

BOOTH, J. S., O'LEARY, D. W., POPENOE, P. & DANFORTH, W. W. 1993. U.S. Atlantic continental slope landslides: Their distribution, general attributes, and implictions. *In:* SCHWAB, W. C., LEE, H. J. & TWICHELL, D. C. (eds) *Submarine Landslides: Selected Studies in the US Exclusive Economic Zone*. USGS Bulletin 2002, 14–22.

BUGGE, T., BELDERSON, R. H. & KENYON, N. H. 1988. The Storegga slide. *Transactions of the Royal Society of London*, **325**, 357–388.

CARLSON, P. R., KARL, H. A., EDWARDS, B. D. & GARDNER, J. V. 1993. Mass movement related to large submarine canyons along the Beringian margin, Alaska. *In:* SCHWAB, W. C., LEE, H. J. & TWICHELL, D. C. (eds) *Submarine Landslides: Selected Studies in the US Exclusive Economic Zone*. USGS Bulletin 2002, 104–116.

COULTER, H. W. & MIGLIACCIO, R. R. 1966. *Effects of the earthquake of March 27, 1964, at Valdez, Alaska*. US Geological Survey Professional Paper **542–C**, 36.

DILLON, W. P., RISCH, J. S., SCANLON, K. M., VALENTINE, P. C. & HUGGETT, Q. J. 1993. Ancient crustal fractures control the location and size of collapsed blocks at the Blake Escarpment, east of Florida. *In:* SCHWAB, W. C., LEE, H. J. & TWICHELL, D. C. (eds) *Submarine Landslides: Selected Studies in the US Exclusive Economic Zone*. US Geological Survey Bulletin 2002, 54–59.

DIMAKIS, P., ELVERHØI, A., HØEG, K., SOLHEIM, A., HARBITZ, C., LABERG, J. S., VORREN, T. O. & MARR, J. 2000. Submarine slope stability on high-latitude glaciated Svalbard-Barents Sea margin. *Marine Geology*, **162**, 303–316.

DOWDESWELL, J. A., KENYON, N. H. & LABERG, J. S. 1997. The glacier influenced Scoresby Sund Fan, East Greenland continental margin: evidence from GLORIA and 3.5 kHz records. *Marine Geology*, **143**, 207–221.

EDGERS, L. & KARLSRUD, K. 1981. *Stability Evaluations for Submarine Slides: Viscous Analysis of Soil Flows Generated by Submarine Slides and Quick-Clay Slides*. Norwegian Geotechnical Institute Report 52207–8, 14.

EDGERS, L. & KARLSRUD, K. 1982. Soil flows generated by submarine slides – case studies and consequences. *In:* CHRYSSOSTOMIDIS, C. & CONNOR, J. J. (eds) *Proceedings of the Third International Conference on the Behaviour of Offshore Structures*. Hemisphere, Bristol, 425–437.

EDWARDS, B. D., LEE, H. J. & FIELD, M. F. 1993. Seismically induced mudflow in Santa Barbara Basin, California. *In:* SCHWAB, W. C., LEE, H. J. & TWICHELL, D. C. (eds) *Submarine Landslides: Selected Studies in the US Exclusive Economic Zone*. USGS Bulletin 2002, 167–175.

ELVERHØI, A., NOREM, H., ANDERSEN, E. S., DOWDESWELL, J. A., FOSSEN, I., HAFLIDASON, H., KENYON, N. H., LABERG, J. S., KING, E. L., SEJRUP, H. P., SOLHEIM, A. & VORREN, T. 1997. On the

origin and flow behaviour of submarine slides on deep-sea fans along the Norwegian-Barents Sea continental margin. *Geo-Marine Letters*, **17**, 119–125.

FAIRCHILD, L. H. & WIGMOSTA, M. 1983. Dynamic and volumetric characteristics of the 18 May 1980 lahars on the Toutle River, Washington. *In: Proceedings of the Symposium on Erosion Control in Volcanic Areas.* Technical Memoir 108, Japanese Public Works Research Institute, Tokyo, pp. 131–153.

FOSSEN, I. 1996. *Stability and Geotechnical Properties of Glacial Sediments on the Western Svalbard Continental Slope.* Masters' thesis, University of Oslo (in Norwegian).

GEE, M. J. R., MASSON, D. G., WATTS, A. B. & ALLEN, P. A. 1999. The Saharan debris flow: an insight into the mechanics of long runout submarine debris flows. *Sedimentology*, **46**, 317–355.

GUTMACHER, C. E. & NORMARK, W. R. 1993. Sur Submarine Slide, a Deep-Water Sediment Slope Failure. *In:* SCHWAB, W. C., LEE, H. J. & TWICHELL, D. C. (eds) *Submarine Landslides: Selected Studies in the US Exclusive Economic Zone.* USGS Bulletin, 2002, 158–166.

HAMPTON, M. A., LEMKE, R. W. & COULTER, H. W. 1993. Submarine landslides that had a significant impact on man and his activities: Seward and Valdez, Alaska. *In:* SCHWAB, W. C., LEE, H. J., & TWICHELL, D. C. (eds) *Submarine Landslides: Selected Studies in the US Exclusive Economic Zone.* USGS Bulletin, 2002, 123–134.

HAMPTON, M. A., LEE, H. J. & LOCAT, J. 1996. Submarine slides. *Reviews of Geophysics*, **34**, 33–59.

HARBITZ, C. A., PARKER, G., ELVERHØI, A., MARR, J. M., MOHRIG, D. & HARFF, P. in press. Hydroplaning of subaqueous debris flows and glide blocks. *Journal of Geophysical Research – Oceans.*

HEEZEN, B. C. & EWING, M. 1952. Turbidity currents and submarine slumps and the 1929 Grand Banks earthquake. *American Journal of Science*, **250**, 849–873.

HOLOCOMB, R. T. & SEARLE, R. C. 1991. Large landslides from oceanic volcanoes. *Marine Geotechnology*, **10**, 19–32.

HUANG, X. & GARCIA, M. H. 1998. A Herschel-Bulkley model for mud flow down a slope. *Journal of Fluid* Mechanics, **374**, 305–333.

HUANG, X. & GARCIA, M. H. 1999. Modeling of non-hydroplaning mud flows on continental slopes. *Marine Geology*, **154**, 132–142.

IMRAN, J., HARFF, P. & PARKER, G. 2001. A numerical model of submarine debris flows with graphical user interface. *Computers and Geosciences*, **27**, 717–729.

IVERSON, R. M. 1997. The physics of debris flows. *Reviews of Geophysics*, **35**, 245–296.

IVERSON, R. M. & VALLANCE, J. W. 2001. New views of granular mass flows. *Geology*, **29**, 115–118.

JOHNSON, A. M. 1970. *Physical Processes in Geology.* Freeman, San Francisco.

KING, E. L., SEJRUP, H. P., HAFLIDASON, H., ELVERHØI, A. & AARSETH, I. 1996. Quaternary seismic stratigraphy of the North Sea Fan: glacially-fed gravity flow aprons, hemipelagic sediments, and large submarine slides. *Marine Geology*, **130**, 293–315.

KING, E. L., HAFLIDASON, H., SEJRUP, H. P. & LØVLIE, R. 1998. Glacigenic debris flows on the North Sea Trough Mouth Fan during ice stream maxima. *Marine Geology*, **152**, 217–216.

KVALSTAD, T. J., NADIM, F. & HARBITZ, C. B. 2001. *Deepwater Geohazards: Geotechnical Concerns and Solutions.* 2001 Offshore Technology Conference, Texas.

KVENVOLDEN, K. A. 1994. Natural gas hydrate occurrence and issues. *International Conference On Natural Gas Hydrates*, New York.

LABERG, J. S. & VORREN, T. O. 1995. Late Weichselian submarine debris flow deposits on the Bear Island Trough Mouth Fan. *Marine Geology*, **127**, 45–72.

LABERG, J. S. & VORREN, T. O. 2000. The Traenadjupet Slide, offshore Norway; morphology, evacuation and triggering mechanisms. *Marine Geology*, **171**, 95–114.

LEMKE, R. W. 1967. *Effects of the earthquake of March 27, 1964, at Seward, Alaska.* USGS Professional Paper, **542–E**.

LOCAT, J. 1997. Rheological behavior of fine muds and their flow properties in a pseudo-plastic regime. *In: Proceedings of the First International Conference on Debris-Flow Hazard Mitigation: Mechanics, Prediction, and Assessment.* Water Resources Division, ASCE, 260–269.

LOCAT, J. & LEE, H. J. 2002. Submarine landslides: Advances and challenges. *Canadian Geotecnical Journal*, **39**, 193–212.

MARR, J., ELVERHØI, A., HARFF, P., IMRAN, J., PARKER, G. & HARBITZ, C. B. 2002. Numerical simulation of mud-rich subaqueous debris flows on the glacially active margins of the Svalbard-Barents Sea. *Marine Geology*, **159**, 351–364.

MCCLUNG, D. & SCHAERER, P. 1993. *The Avalanche Handbook.* The Mountaineers, Seattle.

MCGREGOR, B. A., ROTHWELL, R. G., KENYON, N. H. & TWICHELL, D. C. 1993. Salt tectonics and slope failure in an area of salt domes in the northwestern Gulf of Mexico. *In:* SCHWAB, W. C., LEE, H. J. & TWICHELL, D. C. (eds) *Submarine Landslides: Selected Studies in the US Exclusive Economic Zone.* USGS Bulletin, 2002, 92–96.

MOHRIG, D., WHIPPLE, K. X., HONDZO, M., ELLIS, C. & PARKER, G. 1998. Hydroplaning of subaqueous debris flows. *Bulletin of the Geological Society of America*, **110**, 387–394.

MOHRIG, D., ELVERHØI, A. & PARKER, G. 1999. Experiments on the relative mobility of muddy subaqueous and subaerial debris flows and their capacity to remobilize antecedent deposits. *Marine Geology*, **154**, 117–129.

MORTON, D. M. & CAMPBELL, R. H. 1974. Spring mudflows at Wrightwood, southern California. *Quarterly Journal of Engineering Geology*, **7**, 377–384.

NEWMAN, J. N. 1977. *Marine Hydrodynamics.* The Massachusetts Institute of Technology, Cambridge.

NORMARK, W. R., MOORE, J. G. & TORRESAN, M. E. 1993. Giant volcano-related landslides and the development of the Hawaiian Islands. In: SCHWAB, W. C., LEE, H. J. & TWICHELL, D. C. (eds) *Submarine Landslides: Selected Studies in the US Exclusive Economic Zone*. USGS Bulletin 2002, 184–196.

NOREM, H., IRGENS, F. & SCHIELDROP, B. 1987. A continuum model for calculating snow avalanche velocities. *In: Proceedings of Avalanche Formation, Movements and Effects*. Davos, IAHS Publications, **162**, 363–379.

NOREM, H., LOCAT, J. & SCHIELDROP, B. 1990. An approach to the physics and the modeling of submarine flowslides. *Marine Geotechnology*, **9**, 93–111.

PIERSON, T. C. 1980. Erosion and deposition by debris flows at Mt Thomas, North Canterbury, New Zealand. *Earth Surface Processes and Landforms*, **5**, 227–247.

PIERSON, T. C. 1985. Initiation and flow behaviour of the 1980 Pine Creek and Muddy river lahars, Mount St Helens, Washington. *Bulletin of the Geological Society of America*, **96**, 1056–1069.

PIERSON, T. C., JANDA, R. J., THOURET, J. C. & BORRERO, C. A. 1990. Perturbation and melting of snow and ice by the 13 November 1985 eruption of Nevado del Ruiz, Colombia, and consequent mobilization, flow and deposition of lahars. *Journal of Volcanological Geothermal Resources*, **41**, 17–66.

PIPER, D. J. W., COCHONAT, P. & MORRISON, M. L. 1999. The sequence of events around the epicentre of the 1929 Grand Banks earthquake: initiation of debris flows and turbidity current inferred from sidescan sonar. *Sedimentology*, **46**, 79–97.

PLAFKER, G. & ERICKSEN, G. E. 1978. Nevado Huascaran avalanches, Peru. *In:* VOIGT, B. (ed.) *Rockslides and Avalanches*. Vol. 1, Natural Phenomena. Elsevier, Amsterdam, 277–314.

POPENOE, P., SCHMUCK, E. A. & DILLON, W. P. 1993. The Cape Fear landslide: Slope failure associated with salt diapirism and gas hydrate decomposition. *In:* SCHWAB, W. C., LEE, H. J. & TWICHELL, D. C. (eds) *Submarine Landslides: Selected Studies in the US Exclusive Economic Zone*. US Geological Survey Bulletin 2002, pp.40–53.

PRIOR, D. B. & COLEMAN, J. M. 1982. Submarine landslides – geometry and nomenclature. *Zeitschrift für Geomorphology* N.F., **23**, 415–426.

SAVAGE, S. B. & HUTTER, K. 1989. The motion of a finite mass of granular material down a rough incline. *Journal of Fluid Mechanics*, **199**, 177–215.

SCHEIDEGGER, A. E. 1973. On the prediction of the reach and velocity of catastrophic landslides. *Rock Mechanics*, **5**, 231–236.

SCHLICHTING, H. 1968. *Boundary Layer Theory*. McGraw-Hill, New York.

SCHWAB, W. C. & LEE, H. J. 1993. Processes controlling the style of mass movement in glaciomarine sediment: Northeastern Gulf of Alaska. *In:* SCHWAB, W. C., LEE, H. J. & TWICHELL, D. C. (eds) *Submarine Landslides: Selected Studies in the US Exclusive Economic Zone*. USGS Bulletin 2002, 135–142.

SHARP, R. P. & NOBLES, L. H. 1953. Mudflow of 1941 at Wrightwood, southern California. *Bulletin of the Geological Society of America*, **64**, 547–560.

SIMPSON, J. E. 1987. *Gravity Currents: In the Environment and the Laboratory*. Ellis Horwood Ltd., Chichester, England.

SOLHEIM, A., FALEIDE, J. I., ANDERSEN, E. S., ELVERHØI, A., FORSBERG, C. F., VANNESTE, K., UENZELMANN-NEBEN, G. & CHANNELL, J. E. T. 1998. Late Cenozoic seismic stratigraphy and glacial geological development of the East Greenland and Svalbard-Barents Sea continental margins. *Quaternary Science Reviews*, **17**, 155–184.

VALLANCE, J. W. & SCOTT, K. M. 1997. The Osceola mudflow from Mount Rainier: Sedimentology and hazard implications of a huge clay-rich debris flow. *Bulletin of the Geological Society of America*, **109**, 143–163.

VORREN, T. O., BLAUME, F., DOWDESWELL, J. A., LABERG, J. S., MIENERT, J., RUMOHR, J. & WERNER, F. 1998. The Norwegian-Greenland Sea continental margins: morphology and late Quaternary sedimentary processes and environments. *Quaternary Science Reviews*, **17**, 273–302.

WIECZOREK, G. F., HARP, E. L., MARK, R. K. & BHATTACHARYA, A. K. 1988. Debris flows and other landslides in San Mateo, Santa Cruz, Contra Costa, Alameda, Napa, Solano, Sonoma, Lake and Yolo counties and factors influencing debris-flow distribution. *In:* ELLEN, S. D. & WIECZOREK, G. F. (eds) *Landslides, Floods and Marine Effects of the Storm of January 3–5, 1982, in the San Francisco Bay Region, California*. US Geological Survey Professional Paper, 1434, 133–162.